Mullite formation kinetic from a porcelain stoneware body for tiles production

M. Romero, J. Martín-Márquez and J.Ma. Rincón
Group of Glassy and Ceramic Materials, Instituto de Ciencias de la Construcción Eduardo Torroja, CSIC. C/ Serrano Galvache 4, 28033 Madrid, Spain.

Abstract
The growth of mullite ($3Al_2O_3 \cdot 2SiO_2$) in a porcelain stoneware body for tiles production has been investigated using differential thermal analysis (DTA). The activation energy calculated by both isothermal and non-isothermal treatments is 599 and 622 kJ mol^{-1} respectively. The growth morphology parameters n and m are both about 1.5 indicating that bulk nucleation is dominant in mullite crystallization followed by three-dimensional growth of mullite crystals with polyhedron-like morphology controlled by diffusion from a constant number of nuclei. The frequency factor calculated by the isothermal treatment is equal to 8.21 x 10^{22} s^{-1}.

Keywords: Mullite, Porcelain stoneware, Growth kinetics, DTA analysis, Ceramic Tile

1. Introduction

Porcelain stoneware tile is a highly vitrified ceramic material produced from a body formulated by mixtures of clay, quartz and feldspar in which vitrification indicates a high degree of melting on firing which confers low (often <0.5%) porosity and high (>40%) glass content. The main phase composition of porcelain stoneware body is constituted by a heterogeneous glassy matrix and needle-shaped mullite crystals together with some quartz grains and closed irregular shaped porosities due to gas bubbles. Mullite crystals, which are derived from the solid-state decomposition of the clay component[1], are endowed with excellent mechanical, creep, thermal and chemical properties. Nevertheless, in spite of the commercial interest developed by porcelain stoneware tiles in the last years, very little research has been conducted in this field, leaving significant opportunities for investigation.

Because of its potentially favourable properties, mullite has a significant role in the technological features of porcelain stoneware tiles. It consequently seems of great interest to determine the kinetic parameters for mullite crystallisation in porcelain stoneware tiles.

In the last years, differential thermal analysis (DTA) has been extensively employed as a rapid and convenient instrument for the study of the kinetics of phase transformation processes and chemical reaction mechanisms. In the field of glass science, this method has been used to investigate crystallisation kinetics in glasses[2, 3], to determine homogeneous crystal nucleation rates[4,5] and to obtain the activation energy for glass crystallisation, assuming that the crystallisation process is a first-order reaction[6].

As for mullite crystallisation, the DTA method has been used in recent years to study the kinetic of mullite formation from aluminium silicate glass fiber[7], diphasic gels[8- 10] and kaolin

ceramics[11, 12] by both isothermal and non-isothermal methods. However, to our knowledge, the crystallisation kinetics and growth mechanism of mullite formation in porcelain stoneware tile bodies have not yet been considered in this regard.

In the present study, the crystallisation kinetics of mullite in porcelain stoneware tiles have been investigated by DTA in order to estimate the activation energy of mullite formation based on isothermal and non-isothermal methods, the growth morphology parameters *n* and *m* and the frequency factor for the reaction of mullite formation.

2. Materials and methods

A standard porcelain stoneware body for tiles production was prepared by mixing 50% kaolinitic clay (EuroArce), 40% feldspar (Rio Pirón) and 10% quartz sand. Chemical analysis of the raw materials is shown in Table 1. All the above materials were crushed, grounded and finally powdered to <160 μm prior to further use. The batch composition was wet-milled with alumina grinding media. The slurry was oven-dried overnight at 100 °C, powdered and sieved through a 160 μm mesh.

Table 1. Chemical analysis of the raw materials used in the preparation of a standard porcelain stoneware body for tiles production

Oxide	Kaolinitic clay	Feldspar	Quartz sand
SiO_2	58.10	70.50	98.00
Al_2O_3	27.60	16.60	1.08
Fe_2O_3	1.58	0.06	0.31
CaO	0.26	0.55	0.08
MgO	0.40	0.06	–
Na_2O	–	2.30	–
K_2O	1.62	10.30	–
TiO_2	0.65	0.05	0.57
MnO	0.01	–	–
P_2O_5	0.16	–	–
I.L.	9.40	0.50	0.28

Differential thermal and thermogravimetric analysis (DTA/TG) was performed on the porcelain stoneware powders in a SETARAM Labsys Thermal Analyser. The samples were heated from room temperature to 1250 °C at heating rates of 10, 20, 30, 40 and 50 °C min^{-1}. The DTA scans were conducted in flowing air using platinum crucibles with calcined Al_2O_3 as reference material. All the DTA curves were normalised with respect to the sample weight.

The morphology of the samples after DTA runs was observed by scanning electron microscopy (SEM) in a JEOL JMS 5400 microscope.

3. Theoretical approach

3.1. Isothermal treatment

The theoretical basis for interpreting DTA results is provided by the Johnson-Mehl-Avrami (JMA) theory, which describes the evolution of the crystallisation fraction, *x*, with the time, *t*, during a phase transformation under an isothermal condition.

$$x = 1 - \exp\left[-(kt)^n\right] \quad (1)$$

where *x* is the volume fraction crystallised after time *t*, *n* the Avrami exponent and *k* the reaction rate constant, whose temperature dependence is generally expressed by the Arrhenian type equation:

$$k = k_0 \exp\left(-E / RT\right) \quad (2)$$

where k_0 is the frequency factor, E is the apparent activation energy, R is the ideal gas constant and T is the isothermal temperature in Kelvin. Taking the logarithm of Eq. (1) and rearranging gives

$$-\ln\left(1-x\right) = \left(kt\right)^n \quad (3)$$

After twice taking the logarithm one obtains

$$\ln\left[-\ln\left(1-x\right)\right] = n\ln k + n\ln t \quad (4)$$

At a given temperature, values of n and k are obtained from an isothermal DTA curve using Eq. (4) by least-squares fitting of ln[-ln(1-*x*)] versus ln *t*. Values of *k* were evaluated at different temperatures by repeating the same procedure. The activation energy, E, and frequency factor k_0, are then evaluated from the logarithmic form of Eq. (2) by least-squares fitting, ln *k* versus 1/T.

The crystallization rate can be expressed by:

$$\frac{dx}{dt} = kf(x) = k_0 \exp\left(-\frac{E}{RT}\right) f(x) \tag{5}$$

and taking logarithms,

$$\ln\left(\frac{dx}{dt}\right) = \ln\left[k_0 f(x)\right] - \frac{E}{RT} \tag{6}$$

These equations have been derived for isothermal crystallization process but it has been proved that with certain restrictions[13] they can be applied to non-isothermal experiments with satisfactory results.

Ligero et al.[14] have proposed a mathematical method through non-isothermal techniques. The crystallization fraction, *x*, at a temperature *T* differs at different heating rates and hence, the curves of d*x*/d*t* versus temperature are also different. If we select the same value of *x* in every experiment at different heating rates, there should be a linear relationship between the corresponding d*x*/d*t* and 1/T, whose slope gives the activation energy, *E*. Then, it is possible to calculate, through Eq. (6), the value of ln[k_0 *f(x)*] for each crystallized fraction at each heating rate. From the plot of ln[k_0 *f(x)*] versus *x*, we can select many pairs of x_1 and x_2 that satisfied the condition

$$\ln\left[k_0 f(x_1)\right] = \ln\left[k_0 f(x_2)\right] \tag{7}$$

and therefore,

$$\ln(1-x_1) + \frac{n-1}{n}\ln\left[-\ln(1-x_1)\right] = \ln(1-x_2) + \frac{n-1}{n}\ln\left[-\ln(1-x_2)\right] \tag{8}$$

From Eq. (8) the Avrami parameter, *n*, can be calculated by,

$$n = \ln\left[\ln(1-x_2)/\ln(1-x_1)\right] / \ln\left[\frac{(1-x_2)\ln(1-x_2)}{(1-x_1)\ln(1-x_1)}\right] \tag{9}$$

and once the Avrami parameter is determined, the frequency factor, k_0, can also be calculated by the following equation:

$$\ln\left[k_0 f(x)\right] = \ln k_0 + \ln n + \ln(1-x) + \frac{n-1}{n}\ln\left[-\ln(1-x)\right] \tag{10}$$

Non-isothermal treatment

In a non-isothermal DTA experiment, the temperature is changed linearly with time at a known scan rate ϕ (= dT/d*t*)

$$T = T_0 + \phi t \tag{11}$$

where T_0 is the starting temperature, and T is the temperature after time, *t*. As the temperature constantly changes with time, *k* is no longer a constant but varies with time in a more complicated form, and Eq. (1) becomes

$$x = 1 - \exp\left\{-\left[k(T - T_0)/\phi\right]^n\right\} \tag{12}$$

If the rate of transformation is maximum at the DTA curve peak, then $T=T_p$ and

$$d^2x/dt^2 = 0 \tag{13}$$

After deducing and rearranging Eq. (12), Bansal et al. developed a method for a non-isothermal analysis[15]. The final relation was as follows:

$$\ln\left(T_p^2/\phi\right) = \ln(E/R) - \ln k + E/RT_p\,. \tag{14}$$

A plot of $\ln(T_p^2/\phi)$ versus $1/T_p$ should yield a straight line whose slope and intercept may be used to calculate E and *k*, respectively. The value of the Avrami exponent, *n*, is determined from the shape of the crystallisation exotherm and is related to T_p as[16, 17]

$$n = \frac{2.5}{\Delta T} \times \frac{T_p^2}{E/R} \tag{15}$$

where ΔT is the width of crystallisation peak at half maximum.

Another kinetic approach commonly used to analyse DTA data is the Kissinger method, which is written as

$$\ln\left(\frac{\phi}{T_p^2}\right) = -\frac{E}{RT_c} + const \tag{16}$$

where T_p is the temperature at the maximum of crystallisation peak and ϕ is the DTA heating rate. A plot of $\ln(\phi/T_p^2)$ versus $1/T_p$ should be a straight line, whose slope yields the activation energy for crystallisation, E.

Mattusita and Sakka[18-20] have proposed a modified form of the Kissinger equation as

$$\ln\left(\frac{\phi^n}{T_p^2}\right) = -\frac{mE}{RT_p} + const \qquad (17)$$

where n is the Avrami parameter which indicates the crystallization mode and m is a numerical factor which depends on the dimensionality of crystal growth. The values of n and m for various crystallisation mechanisms obtained by Matusita and Komatsu[21] are shown in Table 2.

Table 2. Values of n and m for various crystallisation mechanisms

	Three-dimensional (polyhedron)		**Two-dimensional (plates)**		**One-dimensional (needles)**	
	n	***m***	***n***	***m***	***n***	***m***
Bulk nucleation with varying number of nuclei						
Interface reaction	4	3	3	2	2	1
Diffusion	2.5	1.5	2	1	1.5	0.5
Bulk nucleation with constant number of nuclei						
Interface reaction	3	3	2	2	1	1
Diffusion	1.5	1.5	1	1	0.5	0.5
Surface nucleation						
Interface reaction	1	1	1	1	1	1
Diffusion	0.5	0.5	0.5	0.5	0.5	0.5

4. Results and discussion

Fig. 1 shows the typical DTA/TG curves recorded on a porcelain stoneware tile powder during heating from room temperature to 1250 °C at a heating rate of 10 °C min^{-1}. In the DTA scan, two endothermic peaks at 520 and 567 °C and a exothermic peak at 984 °C are observed. The TG curve shows a single weight loss of 4.5% correlating with the first endothermic reaction, which corresponds to the dehydroxylation of the kaolinitic clay. The second endothermic and the exothermic peaks, which correspond to the $\alpha \rightarrow \beta$ quartz inversion and mullite formation, respectively, occur without weight loss.

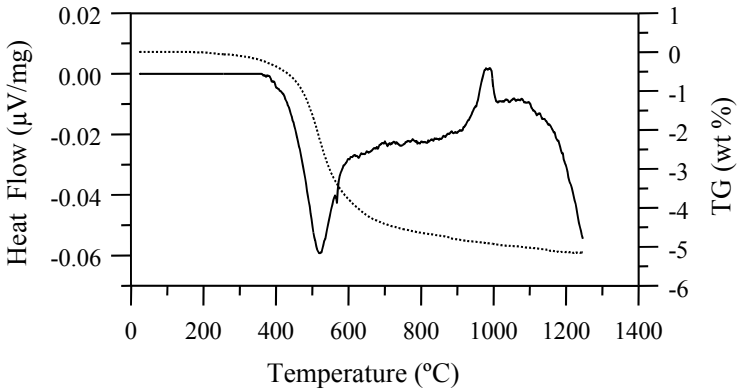

Fig. 1. DTA/TG curves of a porcelain stoneware tile powder heated at 10 °C min^{-1}.

Fig. 2 depicts the DTA curves for a porcelain stoneware tile powder at different heating rates. The temperature of the maximum of the exothermic peak, T_p, shifts to a higher temperature as the heating rate increases from 10 to 50 °C min^{-1}.

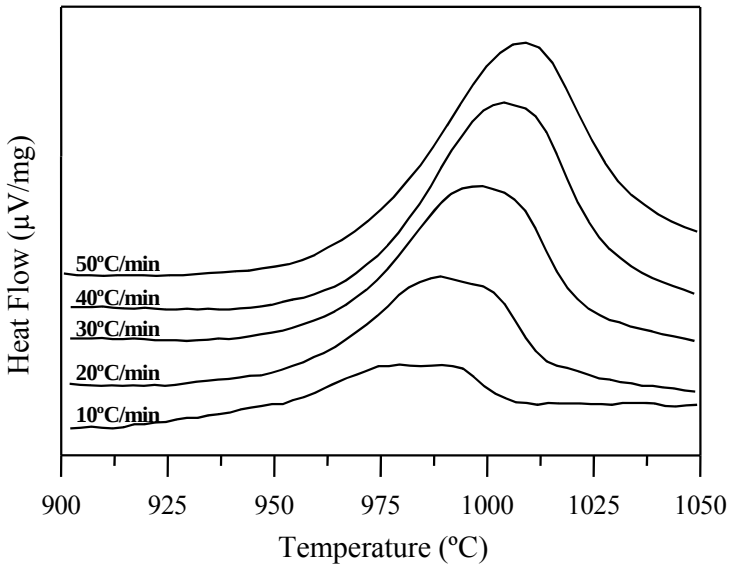

Fig. 2. DTA curves for a porcelain stoneware tile powder at different heating rates.

Fig. 3 shows the variation of the crystallised fraction of mullite with temperature under different heating rates. The crystallised fraction, *x*, was determined from the DTA results (Fig. 2) by the ratio:

$$x = \frac{A_T}{A}$$

where A_T is the area of the exotherm peak in the DTA curve at temperature *T* and *A* is the total area under the peak.

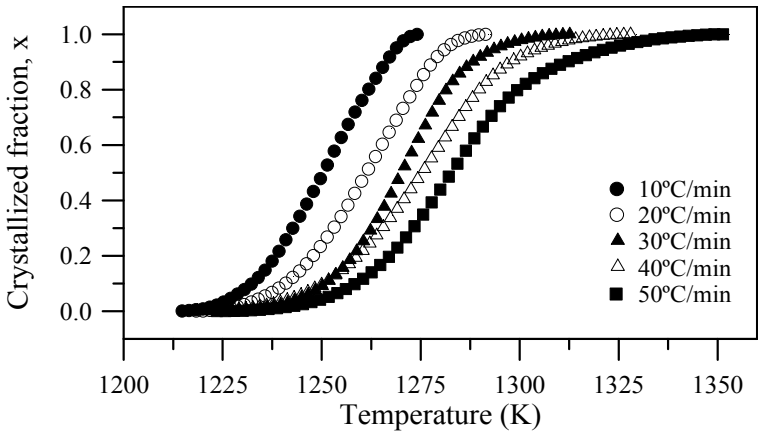

Fig. 3. Variation of the crystallised fraction of mullite with temperature for a porcelain stoneware

As expected, the crystallisation fraction, *x*, at a temperature *T* differs at different heating rates and hence the curves of d*x*/d*t* versus time are also different as is shown in Fig. 4, which depicts the rate of mullite growth with time for different heating rates. The rate of crystallisation increases with the heating rate.

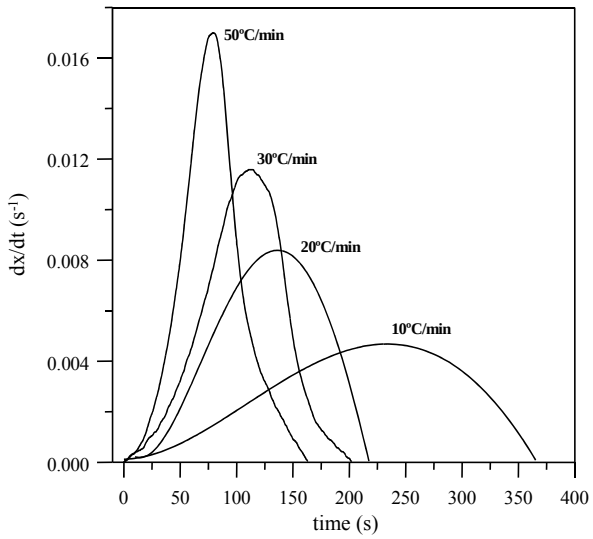

Fig. 4. Rate of mullite growth with time for a porcelain stoneware tile powder at different heating rates.

4.1. Isothermal treatment

Fig. 5 shows the plot of ln(dx/dt) versus 1/T at the same value of crystallised fraction, x, from the experiments at different heating rates as proposed by Ligero et al[14]. The values of the activation energy, E, for different crystallised fraction, which were calculated by the average of the slopes of the lines, are listed in Table 3. It can be seen that ln(dx/dt) is linear with the absolute temperature inverse, independent of the heating rate, in the range $x = 0.11–0.32$ (determination coefficient $r > 0.99$) and the average activation energy of mullite crystallisation in porcelain stoneware is 599 ± 6 kJ mol^{-1}.

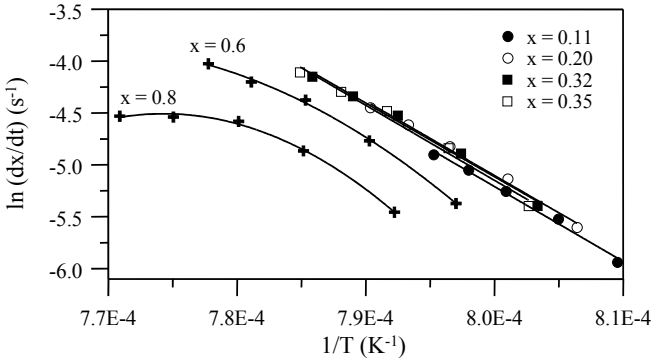

Fig. 5. Plot of ln(dx/dt) vs. 1/T at the same value of crystallised fraction, x, from the experiments at different heating rates.

Table 3. Values of the activation energy, E, for different crystallised fraction

x	r	E (kJ mol^{-1})
0.10	0.987	616
0.11	0.992	601
0.12	0.993	609
0.15	0.994	600
0.20	0.993	597
0.30	0.992	596
0.32	0.991	591
0.35	0.988	601
0.40	0.986	599

Once the activation energy is known, the value of ln[$k_0 f(x)$] can be calculated. Fig. 6 shows the plot of ln[$k_0 f(x)$] versus crystallisation fraction, x, for a porcelain stoneware tile powder heated at a heating rate of 40 °C min^{-1}. Similar curves were obtained for the other heating rates utilized in this work. The Avrami parameter, n, was determined by the selection of many pairs of x_1 and x_2 that satisfied the condition ln[$k_0 f(x_1)$] = ln[$k_0 f(x_2)$]. The average values of n for each heating rate are listed in Table 4 and the average Avrami parameter is 1.39. This value is close

to 1.5, which suggests, according to Table 2, that the crystallisation process of mullite in porcelain stoneware should be controlled by a diffusion growth. Using Eq. (10), the average of k_0 is determined as equal to 8.21×10^{22} s^{-1}.

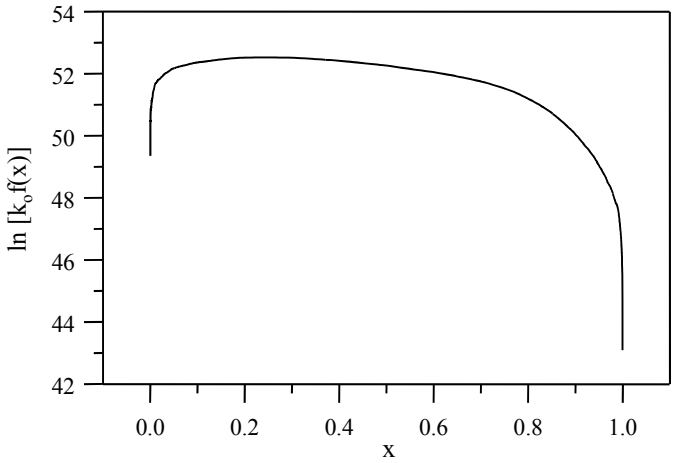

Fig. 6. Plot of $\ln[k_0 f(x)]$ vs. crystallisation fraction, x, for a porcelain stoneware tile powder heated at a heating

The morphology of the crystal growth can be indicated by taking the ratio of times for two fixed degrees of transformation. A convenient representative index is the ratio of times for 75 and 25% transformation in such a way that $2.20 \leq t_{0.75}/t_{0.25} \leq 4.82$ for one-dimensional growth (needles), $1.69 \leq t_{0.75}/t_{0.25} \leq 2.20$ for two-dimensional growth (plates) and $1.48 \leq t_{0.75}/t_{0.25} \leq 1.69$ for three-dimensional growth (polyhedron)[9]. The average values of $t_{0.75}/t_{0.25}$ for each heating rate are listed in Table 4. The average value is 1.62, which suggests a three-dimensional growth of mullite crystals in porcelain stoneware bodies. However, it can be seen that the shape of mullite crystals is very dependent on the heating rate, going from a two-dimensional growth for low heating rate (10 °C min^{-1}) to a three-dimensional growth when the heating rate increases.

Table 4. Values of the Avrami parameter, n, and $t_{0.75}/t_{0.25}$ value for different heating rates

Heating rate	**n**	$\mathbf{t_{0.75}/t_{0.25}}$
10ºC/min	1.39	1.85
20ºC/min	1.43	1.66
30ºC/min	1.44	1.55
40ºC/min	1.36	1.53
50ºC/min	1.34	1.50

4.2. Non-isothermal treatment

Fig. 7 shows the plots of $\ln\left(\frac{\phi}{T_p^2}\right)$ and $\ln\left(\frac{\phi^n}{T_p^2}\right)$versus $1/T_p$ according to Kissinger and Matusita equations, respectively. The activation energy calculated from the slope of the Kissinger plot is 622 kJ mol^{-1}, which is in good agreement with that of 599 estimated by the Ligero method. According to Matusita equation, it is found that the parameter *m* is 1.4 for mullite formation in porcelain stoneware bodies. The growth morphology parameters *n* and *m* are both close to 1.5, which is an indication of a three-dimensional growth of mullite crystals with polyhedron-like morphology, which is in agreement with the result obtained by the isothermal treatment. These results also indicate that the bulk nucleation is the dominant mechanism in mullite crystallisation and the crystal growth is controlled by diffusion from a constant number of nuclei as is usual in mullite ceramics[22]. Fig. 8 shows the microstructure observed by SEM on a sample after DTA record at a heating rate of 30 °C min^{-1}.

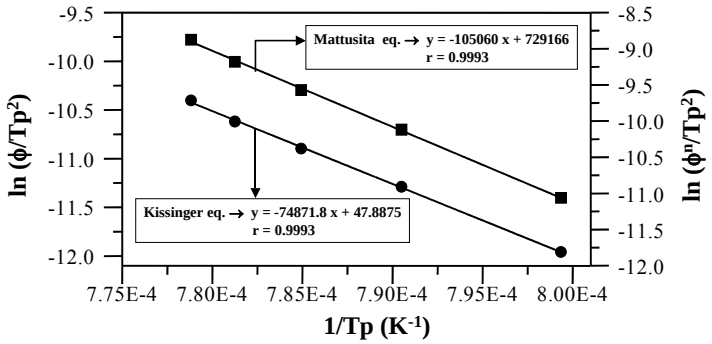

Fig. 7. Plots of $\ln\left(\frac{\phi}{T_p^2}\right)$ and $\ln\left(\frac{\phi^n}{T_p^2}\right)$ vs. $1/T_p$ according to Kissinger and Matusita equations, respectively.

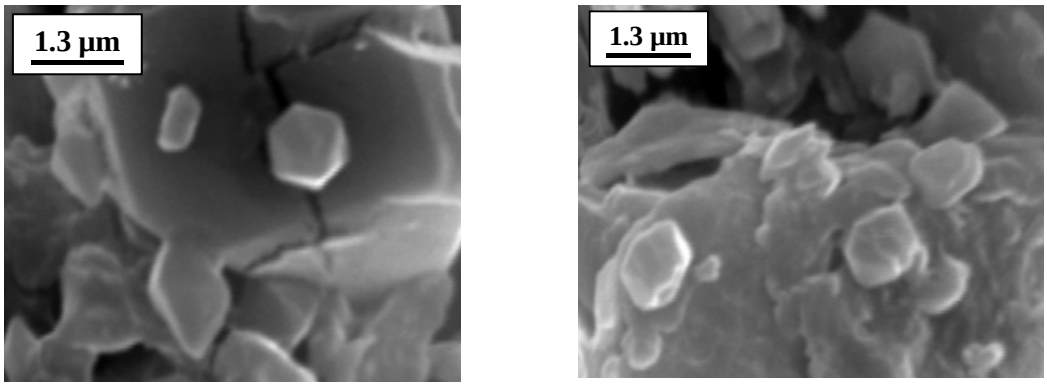

Fig. 8. Microstructure observed by SEM on a sample after DTA record at a heating rate of 30 °C min^{-1}.

5. Conclusions

The crystallisation kinetic and growth mechanism of mullite crystals in a standard porcelain stoneware powder of composition 50% kaolinitic clay, 40% feldspar and 10% quartz for tiles production have been investigate by DTA method. From the experimental results, the following conclusions can be drawn:

• The temperature of mullite crystallisation in the porcelain stoneware powder is around 985 °C

• The activation energies of mullite crystallisation in porcelain stoneware calculated by both isothermal (Ligero method) and non-isothermal (Kissinger method) treatments are 599 and 622 kJ mol^{-1}, respectively.

• The values of the growth morphology parameters n and m are found to be $n = m \approx 1.5$ indicating that bulk nucleation is the dominant mechanism in mullite crystallisation and a three-dimensional growth of mullite crystals with polyhedron-like morphology controlled by diffusion from a constant number of nuclei.

• The value of the frequency factor, k_0, is equal to 8.21×10^{22} s^{-1}.

Acknowledgement

Financial support from the Spanish Science and Technology Ministry (Project MAT2003-02915) is gratefully acknowledged.

References

1. S.P. Chaudhuri and P. Sarkar, Constitution of porcelain before and after heat-treatment. I. Mineralogical composition, *J. Eur. Ceram. Soc.* **15** (1995), pp. 1035–1061.
2. A. Ozturk, Crystallization kinetics of fluorophosphates glasses Part I. Effect of composition and heating rate, *J. Mater. Sci.* **32** (1997), pp. 2623–2627.
3. Y.M. Sung and J.S. Park, Sintering and crystallization of ($SrO{\cdot}SiO_2$)–($SrO{\cdot}Al_2O_3{\cdot}2SiO_2$) glass-ceramics, *J. Mater. Sci.* **34** (1999), pp. 5803–5809.
4. M.C. Weinberg, Interpretation of DTA experiments used for crystal nucleation rate determinations, *J. Am. Ceram. Soc.* **74** (1991), pp. 1905–1909.
5. Y.K. Lee and S.Y. Choi, Controlled nucleation and crystallization in Fe_2O_3–CaO–SiO_2 glass, *J. Mater. Sci.* **32** (1997), pp. 431–436.

6. K. Matusita, S. Sakka and Y. Matsui, Determination of the activation energy for crystal growth by differential thermal analysis, *J. Mater. Sci.* **10** (1975), pp. 961–966.
7. P. Wei and L. Rongti, Crystallization kinetics of the aluminium silicate glass fiber, *Mater. Sci. Eng. A* **271** (1999), pp. 298–305.
8. A.R. Boccaccini, T.K. Khalil and M. Bücker, Activation energy for the mullitization of a diphasic gel obtained from fumed silica and boehmite sol, *Mater. Lett.* **38** (1999), pp. 116–120.
9. A.L. Campos, N.T. Silva, F.C.L. Melo, M.A.S. Oliveira and G.P. Thim, Crystallization kinetics of orthorhombic mullite from diphasic gels, *J. Non-Cryst. Solids* **304** (2002), pp. 19–24.
10. J.L. Holm, Kaolinites–mullite transformation in different Al_2O_3 systems: thermo-analytical studies, *Phys. Chem. Chem. Phys.* **3** (2001), pp. 1362–1365.
11. O. Castelein, B. Soulestin, J.P. Bonnet and P. Blanchart, The influence of heating rate on the thermal behaviour and mullite formation from a kaolin raw material, *Ceram. Int.* **27** (2001), pp. 517–522.
12. Y.F. Chen, M.C. Wang and M.H. Hon, Phase transformation and growth of mullite in kaolin ceramics, *J. Eur. Ceram. Soc.* **24** (2004), pp. 2389–2397.
13. S. Surinach, M.D. Baro, M.T. Clavaguera and N. Clavaguera, Kinetic-study of isothermal and continuous heating crystallization in $GeSe_2$–GeTe–$Sb2Te_3$ alloy glasses, *J. Non-Cryst. Solids* **58** (1983), pp. 209–217.
14. R.A. Ligero, J. Vazques, M. Casas-Ruiz and R. Jiménez-Garay, A study of the crystallization kinetics of some Cu–As–Te glasses, *J. Mater. Sci.* **26** (1991), pp. 211–215.
15. N.P. Bansal, R.H. Doremus, A.J. Bruce and C.T. Moynihan, Kinetics of crystallization of ZrF_4–BaF_2–LaF_3 glass by differential scanning calorimetry, *J. Am. Ceram. Soc.* **66** (1983), pp. 233–238.
16. C.S. Ray, W. Huang and D.E. Day, Crystallization kinetics of a lithia silica glass Effect of sample characteristics and thermal-analysis measurement techniques, *J. Am. Ceram. Soc.* **74** (1991), pp. 60–66.
17. J.A. Augis and J.D. Bennet, Calculation of Avrami parameters for heterogeneous solid-state reactions using a modification of Kissinger method, *J. Therm. Anal.* **13** (1978), pp. 283–292.
18. K. Matusita, S. Sakka and Y. Matsui, Determination of activation energy for crystal growth by differential thermal analysis, *J. Mater. Sci.* **10** (1975), pp. 961–966.
19. K. Matusita and S. Sakka, Kinetic study of the crystallization of glass by differential scanning calorimetry, *Phys. Chem. Glasses* **20** (1979), pp. 81–84.

20. K. Matusita and S. Sakka, Kinetic-study on crystallization of glass by differential thermal-analysis Criterion on application of Kissinger plot, *J. Non-Cryst. Solids* **38–39** (1980), pp. 741–746.
21. K. Matusita, K. Miura and T. Komatsu, Kinetics of on-isothermal crystallization of some fluorozirconate glasses, *Thermochim. Acta* **88** (1985), pp. 283–288.
22. H. Schneider, K. Okada and J.A. Pask, Mullite and Mullite Ceramics, Wiley, Chichester (1994) pp. 111–112